Nondestructive Evaluation of the Three-Dimensional Morphology of Polyethylene/Polystyrene Blends by Thermal Conductivity

ARTICLE *in* MACROMOLECULES · SEPTEMBER 2001

Impact Factor: 5.8 · DOI: 10.1021/ma010716u

2 AUTHORS, INCLUDING:

Hatsuo Ishida
Case Western Reserve University
448 PUBLICATIONS **12,896** CITATIONS

Nondestructive Evaluation of the Three-Dimensional Morphology of Polyethylene/Polystyrene Blends by Thermal Conductivity

Shoji Okamoto and Hatsuo Ishida*

The NSF Center for Molecular and Microstructure of Composites (CMMC), Department of Macromolecular Science, Case Western Reserve University, Cleveland, Ohio 44106-7202

Received April 26, 2001

ABSTRACT: Morphology of polyethylene (PE)/polystyrene (PS) blends has been investigated by measuring their thermal conductivity, which is analyzed with the Okamoto−Ishida equation. The results of the thermal conductivity measurement suggests that the PE/PS blend system can be classified into three regions in terms of morphology. The morphology of the PE/PS blends in each region is investigated by electron microscopy, microthermal analysis, and a selective extraction technique. The observed morphology is consistent with the suggestions from the thermal conductivity of the blends. The phase inversion points and co-continuous region of the PE/PS blend system are determined by applying the Okamoto−Ishida equation to the thermal conductivity of this blend system. It is concluded that the Okamoto−Ishida equation provides a nondestructive evaluation method for the morphology of polymer blends.

Introduction

Blending polymers is an attractive technique to obtain new polymeric materials. Simply mixing proper materials selected from numerous existing polymers has the potential to tailor the properties required. The properties of polymer blends are dependent on the morphology. Therefore, many studies focus on the relationships between the properties and morphology of the polymer blends. In two-phase blends, upon increasing the content of discontinuous phase A in continuous phase B, the morphology of phase A changes from dispersion of nearly spherical drops to progressively interconnected drops and then rods, fibers, and sheets.[1] With a further increase of A over the phase inversion point, A becomes the continuous phase and B the discontinuous phase. At the phase inversion, both A and B can be stable as continuous phase. This morphology is termed co-continuous.

The co-continuity contributes to the advantageous properties, such as high modulus and high impact strength. Phase inversion causes a drastic change in properties.[1] Hence, it is essential to predict the co-continuous region or the phase inversion point of blends. Some equations are proposed to express the condition of phase inversion.[1−4] From the industrial point of view, not only the prediction but also the evaluation of the cocontinuity or phase inversion is important. In particular, nondestructive evaluation is desired because morphology of blends severely affects the properties of final products. However, it is difficult to find a nondestructive evaluation method for the morphology of polymer blends.

Recently, Okamoto and Ishida proposed a theoretical equation that can describe the thermal conductivity of composite materials.[5] It has been confirmed that the Okamoto−Ishida equation can also evaluate the dispersion, orientation, and packing states of the filler particles in composites from their thermal conductivity.[6] Since thermal conductivity is nondestructively measurable, it is expected that this equation provides nondestructive evaluation of the structure of composites. The Okamoto−Ishida equation is theoretically applicable to any two-phase materials so that applying this equation to polymer blends is a natural extension.

In this study, the morphology of polyethylene (PE)/polystyrene (PS) blends is investigated by applying the Okamoto−Ishida equation to the thermal conductivity of the blends. This blend system is worthwhile for the fundamental study of polymer blends because: (1) it has been studied and commercialized for a long time,[7] (2) both materials are economical, and (3) the difference of the thermal conductivity values of these materials is detectable. The co-continuous region and the phase inversion points of the blends are the major concerns of this study.

Theory

The Okamoto−Ishida equation has been derived from the Cheng−Vachon equation.[8] A comparison of these equations has been reported in authors' previous papers.[5,6] Although it has been confirmed that the Okamoto−Ishida equation is applicable to various filled polymers, it has never been applied to polymer blends. In this study, the notation of the Okamoto−Ishida equation is modified in order for this equation to be applicable to the PE/PS blend system.

Okamoto and Ishida's Theory[5,6]. According to Okamoto and Ishida, when the thermal conductivity of the discontinuous phase, k_d, is greater than that of the continuous phase, k_c, that is, $k_d > k_c$, the thermal resistance of a two-phase material, R_e, is represented by the following equation:

$$R_e = [C''(k_d - k_c)\{k_c + B''(k_d - k_c)\}]^{-1/2} \ln \frac{\{k_c + B''(k_d - k_c)\}^{1/2} + \frac{B''}{2}\{C''(k_d - k_c)\}^{1/2}}{\{k_c + B''(k_d - k_c)\}^{1/2} - \frac{B''}{2}\{C''(k_d - k_c)\}^{1/2}} + \frac{1 - B''}{k_c} \quad (1)$$

When $k_d < k_c$,

$$R_e = 2[-C''(k_d - k_c)\{k_c + B''(k_d - k_c)\}]^{-1/2} \tan^{-1} \frac{B''}{2}\left\{\frac{-C''(k_d - k_c)}{k_c + B''(k_d - k_c)}\right\}^{1/2} + \frac{1 - B''}{k_c} \quad (2)$$

10.1021/ma010716u CCC: $20.00
Published on Web 09/15/2001

Table 1. Maximum Packing Fractions[10,11]

shape of particle	type of packing	ϕ_m
spheres	hexagonal close	0.7405
spheres	face centered cubic	0.7405
spheres	body centered cubic	0.60
spheres	simple cubic	0.524
spheres	random loose	0.601
spheres	randem close	0.637
irregular	randem close	~0.637
fibers (L/D[a] = 5)	three dimensinal random	0.52
fibers (L/D[a] = 20)	three dimensional random	0.25
fibers	uniaxial hexagonal close	0.907
fibers	uniaxial simple cubic	0.785
fibers	uniaxial random	0.82

[a] L and D represent length and diameter of the filler, respectively.

Then, the thermal conductivity of the two-phase materials, k_m, is given as the reciprocal of R_e by definition:

$$k_m = \frac{1}{R_e} \tag{3}$$

In these equations, B'' and C'' are represented by the following equations:

$$B'' = \left(\frac{P_d}{P_{d,max}}\right)^{1/2} \tag{4}$$

and

$$C'' = 4\left(\frac{P_{d,max}}{P_d}\right)^{1/2} \tag{5}$$

where P_d represents the volume fraction of the discontinuous phase and $P_{d,max}$ corresponds to the maximum volume fraction of the discontinuous phase in the material. The parameter $P_{d,max}$ reflects the dispersion, orientation, packing states, and shape of the discontinuous phase. The value of $P_{d,max}$ is usually determined by fitting the calculated values to the experimental data. It has been confirmed that $P_{d,max}$ is replaced with the maximum packing fraction, which was introduced by Lewis and Nielsen.[9] Some values of the maximum packing fractions can be theoretically calculated and listed in Table 1.[10,11] If $P_{d,max} = 0.667$, the Okamoto−Ishida equation is identical to the Cheng−Vachon equation.

Modification of Okamoto—Ishida Equation. Unlike filled polymers, polymer blends will undergo a continuous−discontinuous phase inversion upon varying the ratio of components. Therefore, both eqs 1 and 2 are required to represent the thermal conductivity of polymer blends for the whole composition. To distinguish the parameters for eqs 1 and 2, $P_{d,max}$ is replaced by $P_{PE,max}$ or $P_{PS,max}$ in this study. Theoretically, $P_{PE,max}$ represents the maximum volume fraction of the PE when it is filled while keeping the same dispersion state in the blend. Similarly, $P_{PS,max}$ represents the maximum volume fraction of the PS while keeping the same dispersion state in the blend. These values should represent the dispersion state of the discontinuous phase. Therefore, the morphology of the blends can be revealed by checking the value of $P_{PE,max}$ or $P_{PS,max}$.

When the blends have the discontinuous PE phase, eqs 1, 4, and 5 are rewritten as follows:

$$R_e = [C''(k_{PE} - k_{PS})\{k_{PS} + B''(k_{PE} - k_{PS})\}]^{-1/2} \ln \frac{\{k_{PS} + B''(k_{PE} - k_{PS})\}^{1/2} + \frac{B''}{2}\{C''(k_{PE} - k_{PS})\}^{1/2}}{\{k_{PS} + B''(k_{PE} - k_{PS})\}^{1/2} - \frac{B''}{2}\{C''(k_{PE} - k_{PS})\}^{1/2}} + \frac{1 - B''}{k_{PS}} \tag{6}$$

$$B'' = \left(\frac{P_{PE}}{P_{PE,max}}\right)^{1/2} \tag{7}$$

and

$$C'' = 4\left(\frac{P_{PE,max}}{P_{PE}}\right)^{1/2} \tag{8}$$

where k_{PE} and k_{PS} correspond to the thermal conductivity of the PE and PS, respectively, and P_{PE} stands for the volume fraction of the PE.

When the blends have the discontinuous PS phase, eqs 2, 4, and 5 are rewritten as follows:

$$R_e = 2[-C''(k_{PS} - k_{PE})\{k_{PE} + B''(k_{PS} - k_{PE})\}]^{-1/2} \tan^{-1}\frac{B''}{2}\left\{\frac{-C''(k_{PS} - k_{PE})}{k_{PE} + B''(k_{PS} - k_{PE})}\right\}^{1/2} + \frac{1 - B''}{k_{PE}} \tag{9}$$

$$B'' = \left(\frac{P_{PS}}{P_{PS,max}}\right)^{1/2} \tag{10}$$

and

$$C'' = 4\left(\frac{P_{PS,max}}{P_{PS}}\right)^{1/2}, \tag{11}$$

where P_{PS} stands for the volume fraction of the PS. Inevitably, P_{PE} and P_{PS} have the following relationship:

$$P_{PE} = 1 - P_{PS} \tag{12}$$

Experimental Section

The PE used was Petrothene, high-density polyethylene resin, supplied by U.S.I. Chemicals and the PS used was Styron supplied by the Dow Chemical Co. The properties of these materials are listed in Table 2.

The PE and PS were mixed at 170 °C in a Banbury mixer which was connected to Brabender Plasticorder. The mixing was conducted at 16-rpm screw speed for 20 min for each blend. The torque for the PE and PS under mixing conditions was measured by the Brabender Plasticorder. Viscosity of the PE and PS at 170 °C was measured by an automatic capillary rheometer (Monsanto Co.).

Thermal conductivity of the samples was measured with a Holometrix laser flash system, a Microflash 300, which is equipped with a pulsed glass laser with a repetition rate of once per minute. The blended materials were compression molded at 170 °C and cooled to room temperature by a water cooling system. The resulting disk-shaped specimens for the laser flash measurement have ca. 0.8 mm thicknesses and 12.6 mm diameters. The sample specimens were coated with Au/Pd by sputtering in order to avoid the influence of transmitted infrared on the laser flash measurement. The thickness of the Au/Pd coating was 100 nm. Then, they were coated with graphite to increase the signal-to-noise ratio in the measurement of thermal conductivity by the laser flash. The dry graphite spray, dgf123, produced by Miracle Powder Corp., was used to coat the samples. The measurement was carried out

Table 2. Properties of Materials Used

material	density (g/cm^3)	thermal conductivity (W/m·K)
PE	0.954	0.413
PS	1.056	0.146

at room temperature. The Cowan analysis[12] was used for determining the thermal diffusivity of the samples. To obtain the heat capacity of samples, Vespel (polyimide), $C_{p,v} = 1073$ J/kg·K, $\rho_v = 1420$ kg/m^3, and $k_v = 0.379$ W/m·K at 25 °C, was used as a reference sample, where $C_{p,v}$, ρ_v and k_v stand for the heat capacity, density, and thermal conductivity of Vespel, respectively. The obtained values of the heat capacity and the thermal diffusivity for each sample were used for calculating the thermal conductivity of the sample with the following equation

$$k_s = \alpha_s \rho_s C_{p,s}$$

where k_s, α_s, ρ_s, and $C_{p,s}$ are the thermal conductivity, thermal diffusivity, density, and heat capacity of the sample, respectively. At least four sample specimens were used in the measurement for each blend composition, and the average value was adopted as the experimental data.

After the laser flash measurement, some sample specimens were microtomed in cross section at room temperature and, subsequently, their morphology was observed by scanning electron microscopy (SEM) and microthermal analysis. SEM was performed on a JEOL JSM 840 scanning electron microscope and operated at 15 kV in secondary electron imaging mode. The microthermal images were obtained by the μTA 2990 MicroThermal analyzer (TA Instruments, Inc.). The scan rate was 100 μm/s. The probe temperature was fixed at 40 °C.

The crystallinity of the PE in the PE/PS blends was investigated by differential scanning calorimetry (DSC), which was performed on a Modulated DSC 2920 with a heating rate of 5 °C/min under nitrogen purge. The measurement was conducted under standard DSC mode.

The degree of continuity for PE and PS is determined by a selective extraction technique. Tetrahydrofuran (THF) was used as the selective solvent. The sample specimens having the same dimension as the laser flash samples were immersed in THF for at least 2 weeks. Then, the THF solutions were replaced with the new solvent and held for at least additional 1 week. Subsequently, the self-supporting sample specimens were taken out from the solvent and dried under vacuum until their weights became constants. Continuity of the PS was determined as the ratio of the extracted weight of the PS to the original weight of the PS, while the continuity of the PE was determined as the ratio of the residual weight of the PE to the original weight of the PE.

Results and Discussion

Variation of PE Crystallinity in PE/PS Blends. It is reported that crystallinity of PE in PE/PS blends decreases as the PS content increases.[13,14] The change of crystallinity in materials is supposed to cause a variation in the density and thermal conductivity of the materials. Therefore, the crystallinity of the PE in the PE/PS blends was investigated at first. Then, the determined crystallinity of the PE is utilized to evaluate the density and thermal conductivity of the materials.

Figure 1 shows the DSC thermogram of PE/PS = 20/80. The T_g of the PS and the melting peak of the PE are observed around 100 and 129 °C, respectively. The heat of fusion for the PE/PS blend sample is provided by integration of the endotherm between 110 and 140 °C. Since the heat of fusion for PE is known to be 293 J/g,[15] the crystallinity of the PE in the PE/PS blends is determined form their heat of fusion using the following equation

$$X = \Delta H/293, \qquad (13)$$

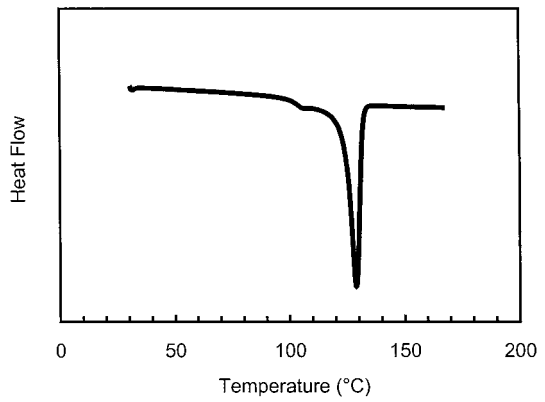

Figure 1. DSC thermograms of PE/PS = 20/80.

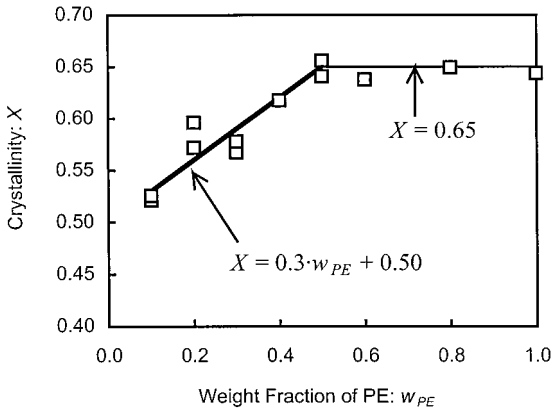

Figure 2. Crystallinity of the PE in the PE/PS blends.

where X stands for the crystallinity of the PE in terms of weight fraction and ΔH(J/g) represents the heat of fusion for the PE.

The crystallinity of the PE is plotted against the weight fraction of the PE in the PE/PS blends in Figure 2. The crystallinity of the PE is almost constant between 0.5 and 1.0 for the weight fraction of the PE while it decreases upon decreasing the PE content below 0.5. The crystallinity change is thought to occur because the presence of PS interferes the crystallization of PE.[13] The truth that the crystallinity of the PE is dependent on the composition should be considered in this research. Therefore, the analysis will be conducted as shown in Scheme 1.

Thermal Conductivity of PE in PE/PS Blends. PE Crystallinity vs Blend Composition. Wycisk et al. reported a monotonic crystallinity change of PE in the PE/PS blend system. However, to simplify the system, it is roughly assumed that the relationship between the crystallinity of the PE and the weight fraction of the PE in the PE/PS blends is represented by the following equations:

$$X = 0.30 w_{PE} + 0.50 \quad \text{when } w_{PE} \le 0.50; \qquad (14)$$

$$X = 0.65 \quad \text{when } w_{PE} > 0.50 \qquad (15)$$

In these equations, w_{PE} represents the weight fraction of the PE in the PE/PS blend. Two linear lines calculated from eqs 14 and 15 are plotted in Figure 2. Although this simplification might be dictatorial, the assigned lines determined by eqs 14 and 15 fit enough to the experimental data. Therefore, using these two lines to represent the relationship between X and w_{PE} would be reasonable in this study.

Scheme 1. Flow Chart of Investigation Process

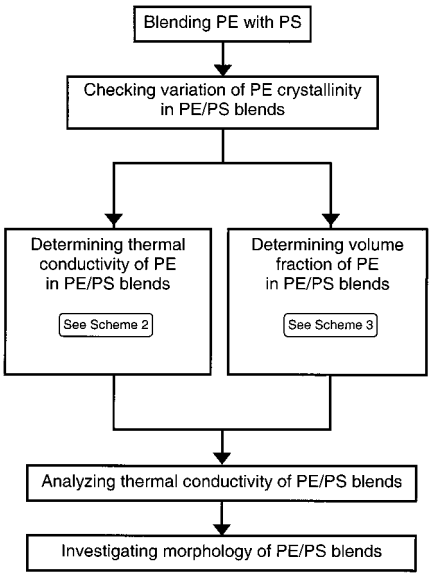

Thermal Conductivity of PE vs PE Crystallinity. The effect of the crystallinity on the thermal conductivity of PE is well investigated by Choy and Young.[16] They applied the Maxwell model to semicrystalline polymers which are considered as two-phase materials composed of crystalline and amorphous phases. Okamoto and Ishida investigated the same system as Choy and Young, and it was concluded that the Okamoto−Ishida equation fit the theoretical thermal conductivity values to the experimental data better than Choy and Young's equation.[17]

Figure 3 shows the crystallinity dependence of the thermal conductivity of PE.[17] The data used is originally reported by Eiermann[18] and rearranged by Choy and Young.[16] The solid line in Figure 3 is the theoretical curve obtained from Okamoto and Ishida's theory, which is represented by the following equations:

$$k_{\mathrm{PE}} = \frac{1}{R_{\mathrm{PE}}} \tag{16}$$

$$R_{\mathrm{PE}} = [C''(k_{\mathrm{e,crys}} - k_{\mathrm{amor}})\{k_{\mathrm{amor}} + B''(k_{\mathrm{e,crys}} - k_{\mathrm{amor}})\}]^{-1/2} \times \ln\frac{\{k_{\mathrm{amor}} + B''(k_{\mathrm{e,crys}} - k_{\mathrm{amor}})\}^{1/2} + \frac{B''}{2}\{C''(k_{\mathrm{e,crys}} - k_{\mathrm{amor}})\}^{1/2}}{\{k_{\mathrm{amor}} + B''(k_{\mathrm{e,crys}} - k_{\mathrm{amor}})\}^{1/2} - \frac{B''}{2}\{C''(k_{\mathrm{e,crys}} - k_{\mathrm{amor}})\}^{1/2}} + \frac{1 - B''}{k_{\mathrm{amor}}} \tag{17}$$

$$B'' = \left(\frac{P_{\mathrm{crys}}}{P_{\mathrm{crys,max}}}\right)^{1/2} \text{ and} \tag{18}$$

$$C'' = 4\left(\frac{P_{\mathrm{crys,max}}}{P_{\mathrm{crys}}}\right)^{1/2} \tag{19}$$

In these equations, R_{PE} represents the thermal resistance of PE and P_{crys} stands for the volume fraction of crystalline phase in PE. These equations are substantially the same as eqs 1, 3, 4, and 5 but the notation has been changed in order to distinguish two kinds of systems: polymer/polymer blends and crystalline/amorphous polymers.

Since the PE crystal has anisotropic thermal conductivity, the effective thermal conductivity of the PE crystal, $k_{\mathrm{e,crys}}$, has been introduced in order to simplify the analysis. The quantity $k_{\mathrm{e,crys}}$ corresponds to the average value of the thermal conductivity of the PE crystals in random dispersion, k_{amor} stands for the thermal conductivity of the amorphous PE phase, and $P_{\mathrm{crys,max}}$ corresponds to the maximum volume fraction of the crystalline phase while keeping the same dispersion state of the crystals in the PE. For the theoretical curve in Figure 3, the values of the parameters are the following: $k_{\mathrm{e,crys}} = 0.56$ (W/m·K), $k_{\mathrm{amor}} = 0.24$ (W/m·K), and $P_{\mathrm{crys,max}} = 0.70$.[17]

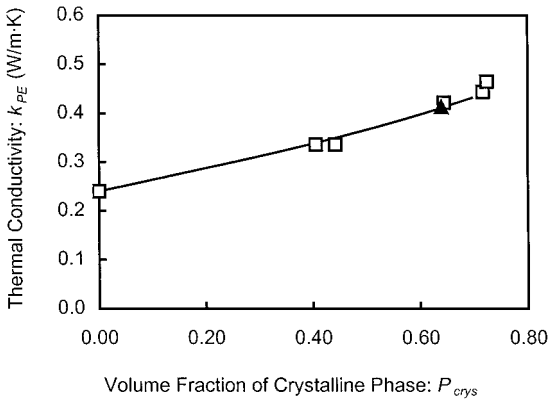

Figure 3. Relationship between thermal conductivity of PE and the volume fraction of the crystalline phase at 300 K. The open squares are experimental data by Eiermann. The closed triangle represents the present PE. The solid line corresponds to the calculated values form eqs 16−19 with $k_{\mathrm{e,crys}} = 0.56$ (W/m·K), $k_{\mathrm{amor}} = 0.24$ (W/m·K), and $P_{\mathrm{crys,max}} = 0.70$.[17]

Scheme 2. Conversion from w_{PE} to k_{PE}

$w_{PE} \longrightarrow X$ by Figure 2 [Equation (14) or (15)]

$X \longrightarrow P_{crys}$ by Equation (20)

$P_{crys} \longrightarrow k_{PE}$ by Figure 3 [Equation (16)-(19)]

The thermal conductivity of the PE used in the present study is also plotted in Figure 3. Since this data point is on the theoretical curve, it would be acceptable to use this theoretical curve for the determination of the thermal conductivity of the present PE in various crystallinity. Therefore, k_{PE} for each PE/PS blend can be determined from w_{PE} by using (a) the theoretical curves in Figure 2 (eq 14 or 15), (b) the theoretical curve in Figure 3 (eqs 16−18), and (c) the following equation

$$P_{\mathrm{crys}} = \frac{X/\rho_{\mathrm{crys}}}{X/\rho_{\mathrm{crys}} + (1 - X)/\rho_{\mathrm{amor}}} \tag{20}$$

where ρ_{crys} and ρ_{amor} represent densities of the crystalline and amorphous phases of PE, respectively. In this study, $\rho_{\mathrm{crys}} = 1.000$ (g/cm^3) and $\rho_{\mathrm{amor}} = 0.879$ (g/cm^3) are applied to be consistent. These values will be explained in detail in the later section. Thermal conductivity of the PE, k_{PE}, is a variable for each volume content of PE and can be determined from the weight fraction of the PE, w_{PE}. The process for obtaining k_{PE} from w_{PE} is illustrated in Scheme 2.

Volume Fraction of PE. Density of PE vs PE Crystallinity. Considering the crystallinity change of the PE, the density of the PE, ρ_{PE}, should also be a variable, which is represented by the following equation:

$$\frac{1}{\rho_{\mathrm{PE}}} = \frac{X}{\rho_{\mathrm{crys}}} + \frac{1 - X}{\rho_{\mathrm{amor}}} \tag{21}$$

Scheme 3. Conversion from w_{PE} to P_{PE}

w_{PE} → X by Figure 2 [Equation (14) or (15)]

X → ρ_{PE} by Equation (21)

ρ_{PE} and w_{PE} → P_{PE} by Equation (22)

Table 3. Properties of PE in PE/PS Blends

sample	w_{PE}	X^a	ρ_{PE} (g/cm^3)^b	$P_{crys}{}^c$	$P_{PE}{}^d$	k_{PE} (W/m·K)^e
PE/PS = 10/90	0.1	0.53	0.939	0.498	0.111	0.362
PE/PS = 20/80	0.2	0.56	0.943	0.528	0.219	0.371
PE/PS = 30/70	0.3	0.59	0.947	0.558	0.323	0.381
PE/PS = 40/60	0.4	0.62	0.950	0.589	0.426	0.390
PE/PS = 50/50	0.5	0.65	0.954	0.620	0.525	0.413
PE/PS = 60/40	0.6	0.65	0.954	0.620	0.624	0.413
PE/PS = 70/30	0.7	0.65	0.954	0.620	0.721	0.413
PE/PS = 80/20	0.8	0.65	0.954	0.620	0.816	0.413
PE/PS = 90/10	0.9	0.65	0.954	0.620	0.909	0.413

[a] From eq 14 or eq 15, and w_{PE}. [b] From eq 21 and X. [c] From eq 20 with ρ_{crys} = 1.000 and ρ_{amor} = 0.879. [d] See Scheme 3. [e] See Scheme 2.

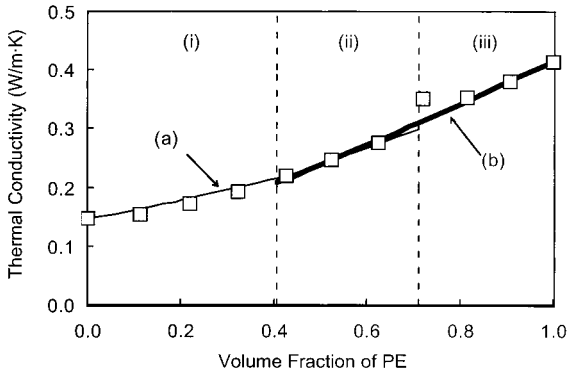

Figure 4. Thermal conductivity of the PE/PS blends. The open squares are experimental data. The solid lines represent the theoretical values calculated from the Okamoto−Ishida equation: (a) $P_{PE,max}$ = 0.712; (b) $P_{PS,max}$ = 0.595. The dotted lines correspond to $P_{PE,max}$ for curve a and $P_{PS,max}$ for curve b.

Since the density of the present PE is 0.954 (g/cm^3) and the crystallinity is 0.65, ρ_{crys} = 1.000 (g/cm^3) and ρ_{amor} = 0.879 (g/cm^3) are applied in order for eq 21 to be consistent. These values are reasonable compared to the reference values: ρ_{crys} = 0.998 − 1.011 (g/cm^3) and ρ_{crys} = 0.811 − 0.8866 (g/cm^3).[19]

Volume Fraction of PE vs Density of PE. The volume fraction of the PE in the PE/PS blend is calculated from the following equation

$$P_{PE} = \frac{w_{PE}/\rho_{PE}}{w_{PE}/\rho_{PE} + (1 - w_{PE})/\rho_{PS}}, \qquad (22)$$

where ρ_{PS} is the density of the PS. From eqs 14, 15, 21, and 22, the volume fraction of the PE in the PE/PS blend is determined by w_{PE}. The process for obtaining P_{PE} from w_{PE} is illustrated in Scheme 3.

The properties of PE blended with PS are listed in Table 3. These values are used in the following analysis of the thermal conductivity data.

Thermal Conductivity of PE/PS Blends. Thermal conductivity of the PE/PS blends is plotted against the volume fraction of the PE in Figure 4. Theoretical curves obtained from eqs 6 and 9 using the values listed in Table 3 are also shown in Figure 4. The value of $P_{PE,max}$ is 0.712 for curve a, and the value of $P_{PS,max}$ is 0.595 for curve b. These values are determined by fitting the calculated values to the experimental data. Figure 4 suggests that there are three regions for this blend system: the regions represented by (i) only curve a, (ii) both curves a and b, and (iii) only curve b. The dotted lines in Figure 1 represent the boundaries of these regions. The boundary of regions i and ii corresponds to $P_{PS,max}$ for curve b, while the boundary of regions ii and iii corresponds to $P_{PE,max}$ for curve a.

In region i, the PS is the predominant component. The morphology of this region is expected to be the PE as the dispersed phase in the PS matrix. Thus, the thermal conductivity of the blends in this region should be obtained from eq 6. In the Okamoto−Ishida equation, the parameter $P_{d,max}$ represents the dispersion, orientation, and packing states of the discontinuous phase. A greater value of $P_{d,max}$ indicates a better dispersion state of the discontinuous phase.[5,6]

For monodispersed spherical particles, the values of maximum packing fraction, which corresponds to $P_{d,max}$, are theoretically between 0.524 and 0.7405 as shown

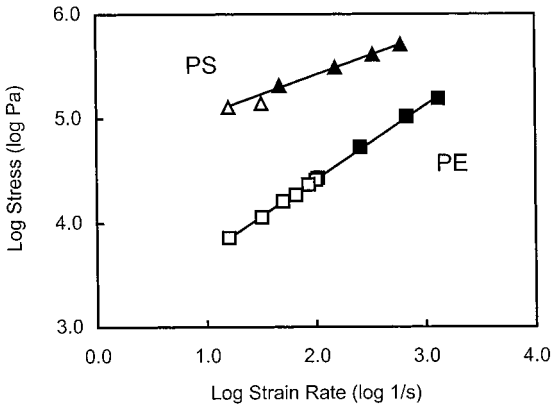

Figure 5. Logarithmic plots of shear stress vs strain ratio for PE and PS. The closed marks are experimental data measured by capillary rheometry. The open marks represent the calculated values from the equations: effective shear stress = k_1 × torque (m·g), k_1 = 120; effective strain rate = k_2 × mixing rate (rpm), k_2 = 1.

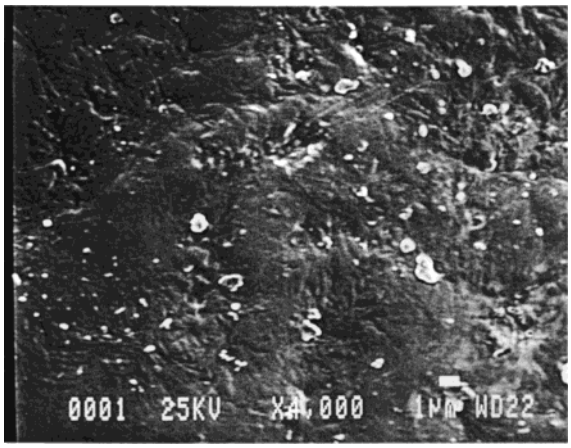

Figure 6. Morphology of PE/PS = 20/80: SEM picture.

Table 4. Viscosity of PE and PS at 170 °C

material	mixing rate (rpm)	torque (m·g)	effective strain rate (1/s)	effective shear stress (Pa)	viscosity (Pa·s)
PE	16	60	16	7200	450
PS	16	1060	16	127200	7950

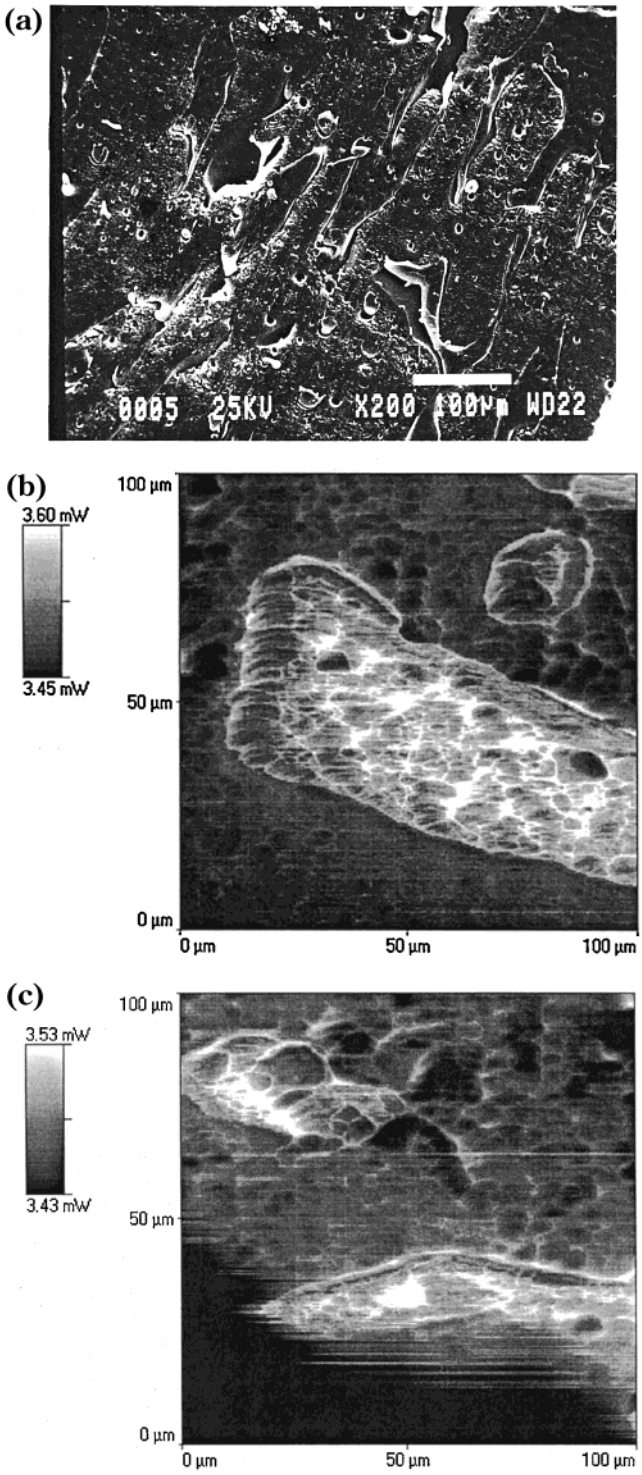

Figure 7. Morphology of PE/PS = 30/70: (a) SEM picture; (b and c) microthermal images.

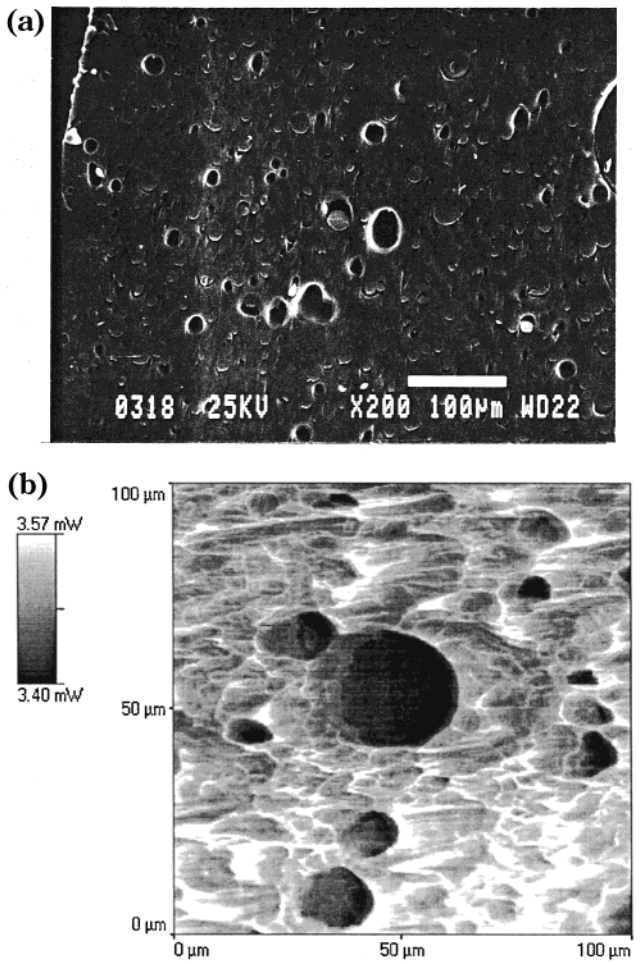

Figure 8. Morphology of PE/PS = 80/20: (a) SEM picture; (b) microthermal image.

in Table 1. Although the size distribution of the minor phase for the present blend system would not be monodisperse, the $P_{PE,max}$ and $P_{PS,max}$ values determined from the thermal conductivity of the blends are considered to be reasonable.

Morphology of PE/PS Blends. The morphology of blends is strongly affected by the viscosity of components during the mixing process.[3,4,20,21] To investigate the viscosity of PE and PS, Miles and Zurek's assumption[4] was used. In this assumption, it can be considered that $\dot{\gamma}_e$ (the effective strain rate) is proportional to R (the applied mixing rate) while σ_e (the effective shear stress) is proportional to T (the measured torque). Therefore, it is possible to superimpose a plot of T vs R on a plot of σ_e vs $\dot{\gamma}_e$ by using the following equations

$$\sigma_e = k_1 T \tag{23}$$

$$\dot{\gamma}_e = k_2 R \tag{24}$$

where k_1 and k_2 are proportionality constants. Figure 5 shows a plot of σ_e vs $\dot{\gamma}_e$ obtained by capillary rheometer and Brabender Plasticorder using eqs 23 and 24. The units used in this study are Pa for σ_e, m·g for T, 1/s for $\dot{\gamma}_e$, and rpm for R. Clearly, the data on the linear lines have been obtained by applying $k_1 = 120$ and $k_2 = 1$. The values of viscosity at mixing condition for the PE and PS are subsequently determined from Figure 5 and listed in Table 4.

The PE has much lower viscosity than the PS under the mixing condition. Danesi and Porter report that better dispersion of the minor phase is achieved when the minor phase has lower viscosity than the major phase.[20] Therefore, the PE phase is supposed to be dispersed very well in the PS phase.

A well-dispersed PE phase is observed in Figure 6, which is the SEM picture of the PE/PS = 20/80. The blend in this composition belongs to region i. The good dispersion of the PE phase in Figure 6 is consistent with the relatively higher value of $P_{PE,max}$ for the curve a in Figure 4 and Danesi and Porter's report.[20]

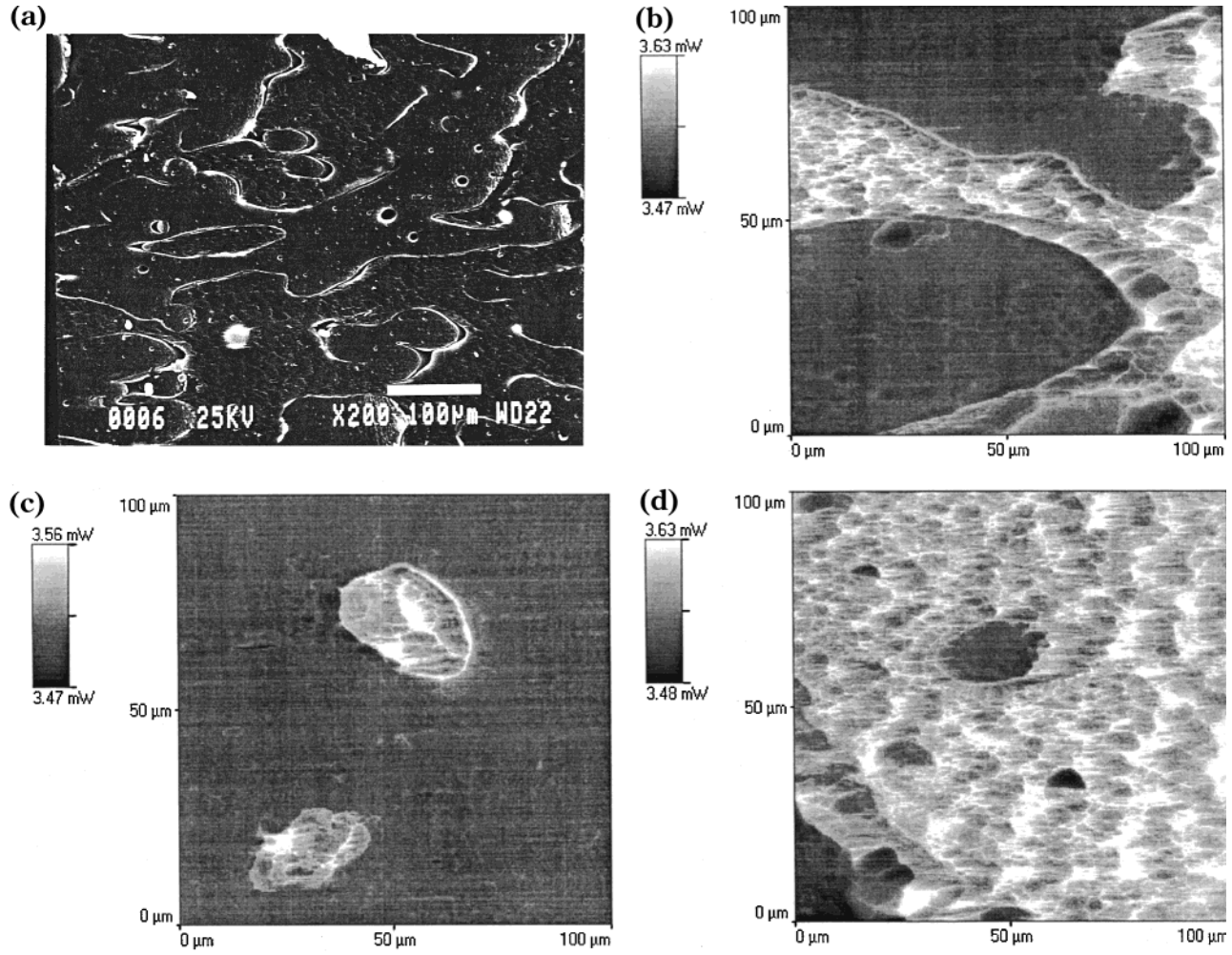

Figure 9. Morphology of PE/PS = 40/60: (a) SEM picture; (b−d) microthermal images.

Figure 7 shows that the morphology of the PE/PS = 30/70, which also belongs to region i. Figure 7a is obtained from SEM, and parts b and c of Figure 7 are the results of microthermal analysis. Since the scale of the dispersed phase of the PE/PS = 30/70 blend is much greater than that of the PE/PS = 20/80 blend, the morphology can be observed by both SEM and microthermal analysis.

In the microthermal images, the brighter area corresponds to the more highly thermally conductive area, which corresponds to the PE phase. Therefore, PE and PS are easily assigned in the microthermal image without staining, unlike in the SEM picture.

Because of the measurement principle, the microthermal images are affected by the topography of the sample. The thermal conductivity of the topographically higher part of the sample has apparently lower thermal conductivity in the microthermal images, and vice versa. Since the sample specimens are microtomed above the T_g of polyethylene and below the T_g of polystyrene, the PE phase has a rougher surface than the PS phase. Therefore, the PE phase has the white "valleys," while the PS phase looks like black "planes" in the microthermal images.

Well mixed PE and PS phases are observed in Figure 7. The PE phase appears well-dispersed in various shapes as if it were a liquid. Large PE lumps can be seen but there are still discontinuous PE lumps in Figure 7. Therefore, only the PS is considered to be the continuous phase. The morphology in Figure 7 looks different from that in Figure 6. However, the dispersion states of the PE phase of both the PE/PS = 20/80 and PE/PS = 30/70 blends must be substantially the same because the thermal conductivity values of both blends are on the same theoretical curve (curve a) in Figure 4.

Before explaining region ii, it would be better to explain region (iii) because this region is similar to region i. In region iii, the PE is the predominant component so that the PS is dispersed in the PE matrix. Therefore, the thermal conductivity of the blends in this region should be obtained from eq 9.

Figure 8 shows the morphology of a blend in region iii. Figure 8a is the SEM picture and Figure 8b is the microthermal image of the PE/PS = 80/20 blend. The spherical PS phase in various sizes and the PE matrix can be clearly distinguished in Figure 8.

As Danesi and Porter indicate, the deformation of the dispersed phase is always less than the deformation imposed on the continuous phase if the minor component has a higher viscosity than the major one.[20] Consequently, the discontinuous phase under this condition cannot be fine and uniform as much as the one under the condition that the dispersed phase has lower viscosity than the continuous phase. Danesi and Porter also mention that the shape of the dispersed phase is more spherical when the dispersed phase has a higher viscosity than the continuous phase.[20] The morphology shown in Figure 8 is consistent with the Danesi and Porter's explanation.

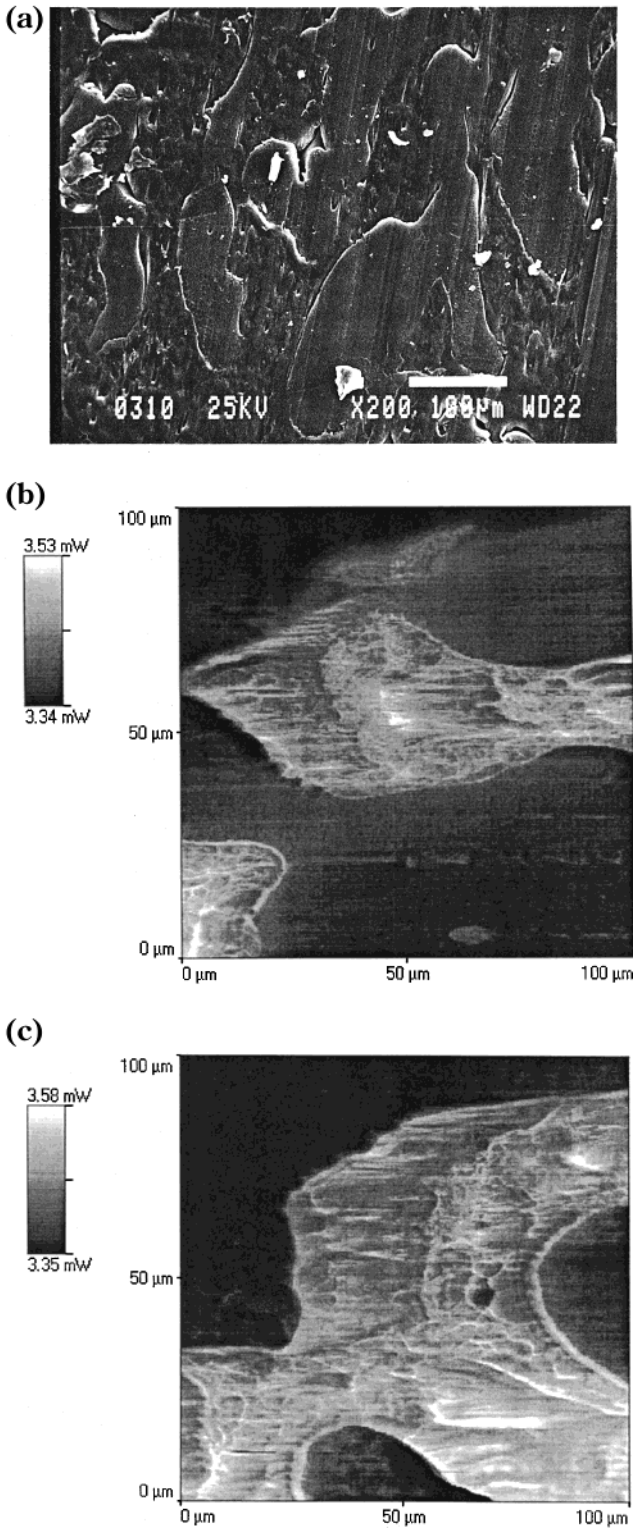

Figure 10. Morphology of PE/PS = 50/50: (a) SEM picture; (b and c) microthermal images.

Region ii, where the volume fraction of the PE is between 0.405 and 0.712, is interesting because the thermal conductivity of the blends in this region can be obtained from both eqs 6 and 9. Simply, it is natural to suggest that this region is co-continuous. From the morphological point of view, co-continuous material is defined as the material that has no discontinuous component.

The morphology of the blends in region ii is shown in Figures 9−11. However, as Lyngaae-Jørgensen and Utracki point out, it is difficult or nearly impossible to evaluate three-dimensional structures from two-dimensional pictures.[21] As they recommend, the selective extraction technique was also utilized to investigate the morphology of the PE/PS blends. This technique gives the degree of continuity of a component.

In Figure 12, the degrees of continuity for the PE and PS components in the PE/PS blends are plotted against the volume fraction of the PE. The dotted lines in Figure 12 correspond to the boundaries of the regions shown in Figure 4. Figure 12 obviously shows that the co-continuous regions, suggested by the selective extraction and thermal conductivity measurement of the blends, are identical. Therefore, it would be reasonable to evaluate the three-dimensional morphology of blends by their thermal conductivity using the Okamoto−Ishida equation.

The morphology and phase inversion of the PE/PS blends are illustrated in Figure 13. When the PE is dispersed in the PS, the PE phase is finely and uniformly dispersed at the lower PE content (Figure 13a). As the PE content increases, the PE is still well-dispersed but has various shapes (Figure 13b). Furthermore, upon increasing the PE phase, some PE lumps are extended through the material continuously and the other PE lumps are still discontinuous (Figure 13c). Then, the PE content reaches the co-continuous region (Figure 13d). In this region, neither the PE nor PS have a discontinuous phase. Exceeding the PE content over the co-continuous region, some PS portions cannot be continuous any longer. Large spherical droplets and the continuous phase of the PS coexist in the blend (Figure 13e). Finally, the continuous PS phase vanishes in the blend (Figure 13f) and the spherical PS droplets, whose sizes are various, are dispersed in the PE matrix (Figure 13g).

Region i in Figure 4 is represented by Figure 13a−c. Only in this region does discontinuous PE exist in the blends. Region iii is represented by Figure 13e−g, and the discontinuous PS exists only in this region. Therefore, the continuous−discontinuous phase inversion of the PE is represented by $P_{PS,max}$, which exists somewhere between parts c and d in Figure 13. The continuous−discontinuous phase inversion of the PS likewise corresponds to $P_{PE,max}$, which exists somewhere between parts d and e in Figure 13.

According to Lyngaae-Jørgensen and Utracki, the critical volume fraction is defined as the volume fraction corresponding to zero extractable weight fraction and is determined by extrapolation from a continuity plot.[21] From Figure 12, the critical volume fractions of the PE, $\phi_{PE,c}$, and PS, $\phi_{PS,c}$, are determined to be 0.22 and 0.14, respectively. Lyngaae-Jørgensen and Utracki report that the critical volume fraction corresponds to a percolation threshold. They showed that $\phi_{PE,c}$ and $\phi_{PS,c}$ were 0.15 and 0.16, respectively. However, these values are not universal, even if the materials of components are the same, because the percolation threshold is dependent on the network of the components as listed in Table 5.[22] This means that the percolation threshold is processing condition dependent.

The critical volume fractions exist somewhere between parts b and c in Figure 13 for $\phi_{PE,c}$ and between parts e and f for $\phi_{PS,c}$. Although percolation is considered to be a phase inversion,[21,23] the percolation threshold is not identical to the continuous−discontinuous phase inversion point.

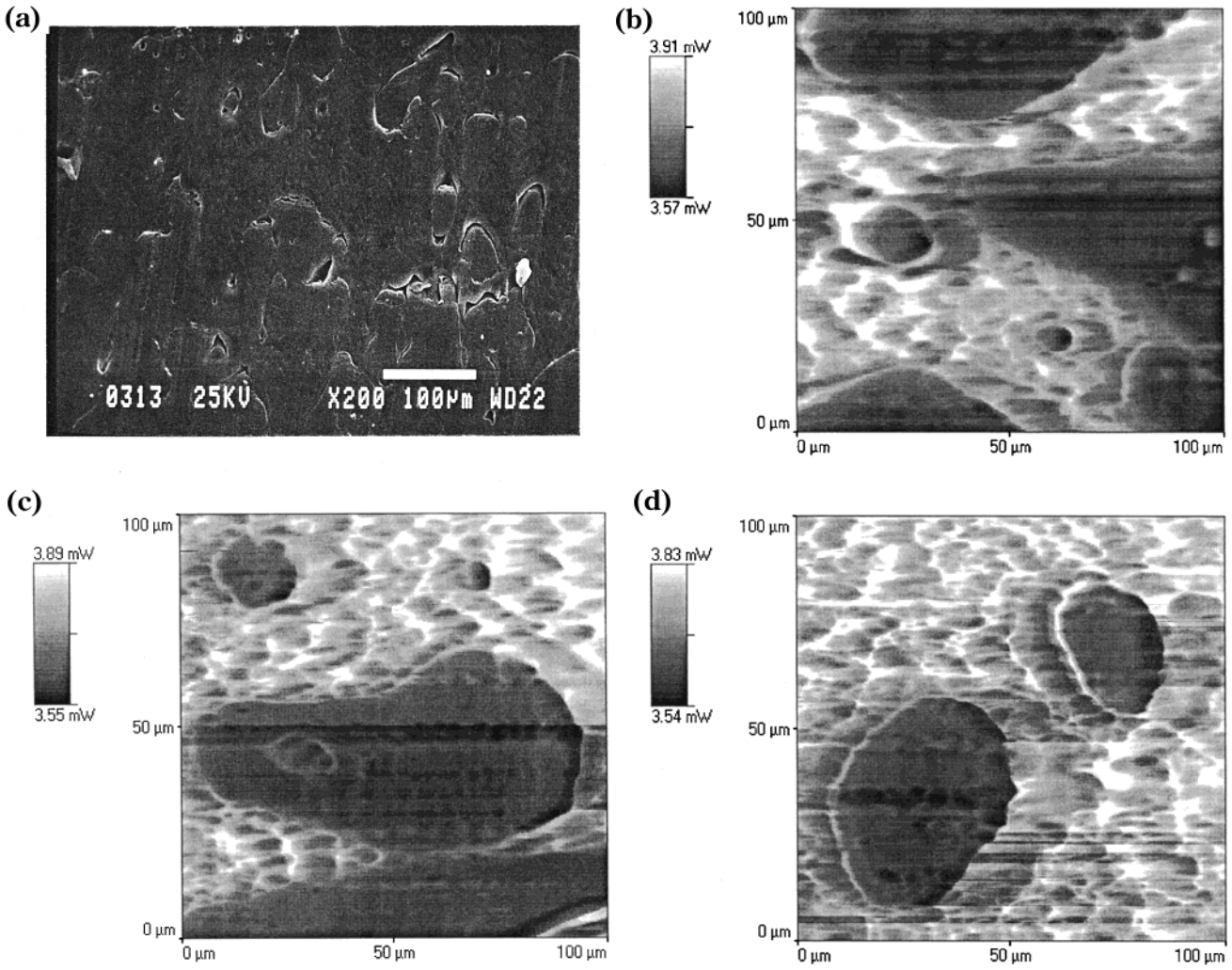

Figure 11. Morphology of PE/PS = 60/40: (a) SEM picture; (b−d) microthermal images.

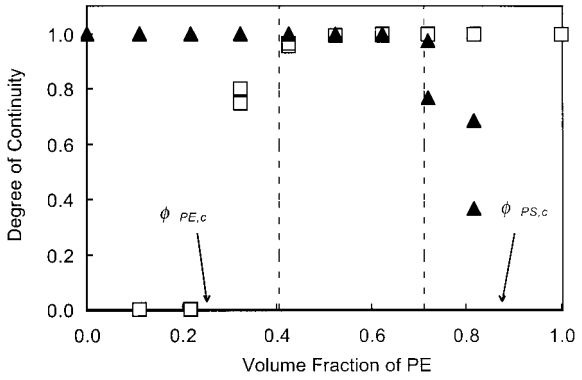

Figure 12. Degree of continuity against volume fraction of PE in blends with PS: the open squares, PE; the closed triangles, PS. The dotted lines correspond to $P_{PE,max}$ for curve b and $P_{PS,max}$ for curve c in Figure 1. $\phi_{PE,c}$ and $\phi_{PS,c}$ are determined by extrapolating the data to zero extractable and remaining weight fraction, respectively.

Several studies confirmed that the phase inversion point is predicted by the following equation:[2−4]

$$\frac{\eta_1}{\eta_2} \cdot \frac{\phi_2}{\phi_1} \cong 1 \tag{25}$$

where η_1 and η_2 represent the viscosity of phases 1 and 2, while ϕ_1 and ϕ_2 represent the volume fraction of phases 1 and 2, respectively. If the quantity in the left term is greater than unity, phase 2 is likely to be continuous. If it is less than unity, phase 1 is likely to be continuous. A co-continuous phase is observed when the quantity is approximately unity. This empirical equation is useful for roughly finding the phase inversion point or co-continuous region of blends. However, it is difficult for this equation to define the exact co-continuous region of blends. From Table 4 and eq 25, the calculated co-continuous region for the PE/PS blend is around $P_{PE} = 0.05$. Yet, as the results of the thermal conductivity measurement and the selective extraction show, the co-continuous region of the PE/PS blend, $0.407 \leq P_{PE} \leq 0.714$, is quite different from the values calculated from eq 25. Such a difference might have been caused by the additional thermal history during the compression molding after mixing process. Since eq 25 represents the morphology of blends during mixing, it may not represent the morphology of molded blends.

On the other hand, the Okamoto−Ishida equation can exactly evaluate the morphology of molded blends from their thermal conductivity. Since the thermal conductivity of the blends is measured after molding, it represents the morphology of the molded blends. Therefore, nondestructive evaluation of the three-dimensional morphology would be possible by the thermal conductivity measurement using the Okamoto−Ishida equation. Evaluation of the morphology of blends is one of the important applications of this equation.

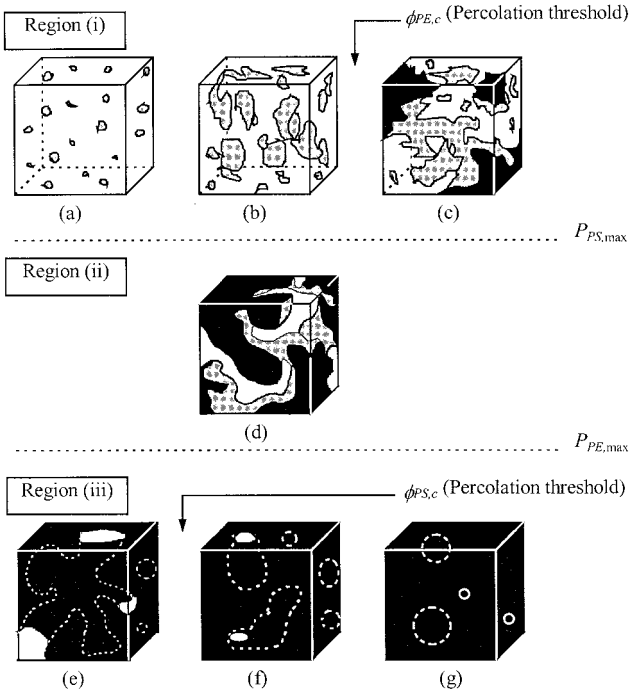

Figure 13. Schematic illustration of PE/PS blends. The black and gray phases represent the PE on the surface and inside of the model cubes, respectively. The white phase represents the PS on the surface of the model cubes. The white dotted lines indicates the PS inside of the model cubes.

Table 5. Percolation Thresholds of Some Three-Dimensional Networks[22]

network	bond percolation threshold	site percolation threshold
diamond	0.3886	0.4299
simple cubic	0.2488	0.3116
body centered cubic	0.1795	0.2464
face centered cubic	0.198	0.119

Conclusions

The morphology of the PE/PS blends has been successfully evaluated from their thermal conductivity by using the Okamoto−Ishida equation. The co-continuous regions suggested by the selective extraction and thermal conductivity of the blends have been identical.

When the volume fraction of the PE is below 0.405, the PE phase is finely and uniformly dispersed in the PS matrix but the shape of the PE phase is various. When the volume fraction of the PE is over 0.712, the PS phase is in spherical shape and dispersed in the PE matrix

The parameters, $P_{PE,max}$ and $P_{PS,max}$, in the Okamoto−Ishida equation represent the continuous−discontinuous phase inversion points. These points are different from the percolation thresholds, which is identical to the critical volume fractions of PE, $\phi_{PE,c}$, and PS, $\phi_{PS,c}$.

The Okamoto−Ishida equation has provided a nondestructive evaluation method for the morphology of polymer blends. This equation is versatile in any heterogeneous material, such as composites and blends.

Acknowledgment. We acknowledge Unitika Ltd., Osaka, Japan, for their financial support of this work. We also thank the support of the NSF Center for Molecular and Microstructure of Composites (CMMC). Furthermore, we thank Dr. S. D. Hudson for letting us operate the equipment for the SEM study.

Nomenclature

$$B'' = \left(\frac{P_d}{P_{d,max}}\right)^{1/2}, \left(\frac{P_{PE}}{P_{PE,max}}\right)^{1/2}, \left(\frac{P_{PS}}{P_{PS,max}}\right)^{1/2} \text{ or } \left(\frac{P_{crys}}{P_{crys,max}}\right)^{1/2}$$

$$C'' = 4\left(\frac{P_{d,max}}{P_d}\right)^{1/2}, 4\left(\frac{P_{PE,max}}{P_{PE}}\right)^{1/2}, 4\left(\frac{P_{PS,max}}{P_{PS}}\right)^{1/2} \text{ or } 4\left(\frac{P_{crys,max}}{P_{crys}}\right)^{1/2}$$

$C_{p,s}$ = heat capacity of sample, J/kg·K
$C_{p,v}$ = heat capacity of Vespel, J/kg·K
k_{amor} = thermal conductivity of amorphous PE, W/m·K
k_c = thermal conductivity of continuous phase, W/m·K
k_d = thermal conductivity of discontinuous phase, W/m·K
$k_{e,crys}$ = effective thermal conductivity of crystalline PE, W/m·K
k_i (i = 1, 2) = proportionality constant in eq 23 or (24)
k_{PE} =thermal conductivity of PE, W/m·K
k_{PS} = thermal conductivity of PS, W/m·K
k_s = thermal conductivity of sample, W/m·K
k_v = thermal conductivity of Vespel, W/m·K
$P_{crys,max}$ = volume fraction of crystalline phase in PE (= crystallinity of PE in terms of volume fraction)
P_d = maximum volume fraction of crystalline phase in PE
P_d = volume fraction of discontinuous phase in two-phase material
$P_{d,max}$ = maximum volume fraction of discontinuous phase
P_{PE} = volume fraction of PE in PE/PS blend
$P_{PE,max}$ = maximum volume fraction of PE
P_{PS} = volume fraction of PS in PE/PS blend
$P_{PS,max}$ = maximum volume fraction of PS
R = applied mixing rate by Banbury mixer, rpm
R_e = thermal resistance of two-phase material, m·K/W
R_{PE} = thermal resistance of PE, m·K/W
T = torque measured by Brabender Plasticorder, m·g
w_{PE} = weight fraction of PE in PE/PS blend
X = crystallinity of PE in terms of weight fraction (= weight fraction of crystalline phase in PE)
α_s = thermal diffusivity of sample, m^2/s
ΔH = heat of fusion, J/g
ϕ_i (i = 1, 2) = volume fraction of phase i
$\phi_{PE,c}$ = critical volume fraction of PE
$\phi_{PS,c}$ = critical volume fraction of PS
$\dot{\gamma}_e$ = effective strain rate, 1/s
η_i (i = 1, 2) = viscosity of phase i, Pa·s
ρ_{amor} = density of amorphous phase in PE, g/cm^3
ρ_{crys} = density of crystalline phase in PE, g/cm^3
ρ_{PE} = density of PE, g/cm^3
ρ_{PS} = density of PS, g/cm^3
ρ_s = density of sample, kg/m^3
ρ_v = density of Vespel, kg/m^3
σ_e = effective shear stress, Pa

References and Notes

(1) Utracki, L. A. *Commercial Polymer Blends*; Chapman & Hall: London, 1998; Chapter 7.
(2) Paul, D. R.; Barlow, J. W. *J. Macromol. Sci., Rev. Macromol. Chem.* **1980**, C18, 109.
(3) Jordhamo, G. M.; Manson, J. A.; Sperling, L. H. *Polym. Eng. Sci.* **1986**, *26*, 517.
(4) Miles, I. S.; Zurek, A. *Polym. Eng. Sci.* **1983**, *23*, 614.
(5) Okamoto, S.; Ishida, H. *J. Appl. Polym. Sci.* **1999**, *72*, 1689.
(6) Okamoto, S.; Ishida, H. *Polym. Compos.*, submitted.
(7) Utracki, L. A. *Commercial Polymer Blends*; Chapman & Hall: London, 1998; Chapter 14.
(8) Cheng, S. C.; Vachon, R. I. *Int. J. Heat Mass Transfer* **1969**, *12*, 249.
(9) Lewis, T. B.; Nielsen, L. E. *J. Appl. Poym. Sci.* **1970**, *14*, 1449.
(10) Nielsen, L. E. *Ind. Eng. Chem., Fundam.* **1974**, *13*, 17.
(11) Bigg, D. M.; *Polym. Comput.* **1986**, *7*, 125.
(12) Cowan, R. D. *J. Appl. Phys.* **1963**, *34*, 926.
(13) Aref-Azar, A.; Hay, J. N.; Marsden, B. J.; Walker, N. *J. Polym. Sci., Polym. Phys. Ed.* **1980**, *18*, 637.
(14) Wycisk, R.; Trochimczuk, W. M.; Matys, J. *Eur. Polym. J.* **1990**, *26*, 535.

(15) Wunderlich, B.; Czornyj, G. *Macromolecules* **1977**, *10*, 906.
(16) Choy, C. L.; Young, K. *Polymer* **1977**, *18*, 769.
(17) Okamoto, S.; Ishida, H. *Polymer*, submitted.
(18) Eiermann, V. K. *Kolloid, Z. Z. Polym*. **1964**, *201*, 3.
(19) Brandrup, J., Immergnt, E. H., Eds.; *Polymer Handbook*, 3rd ed.; John Wiley & Sons Inc.: New York, 1989.
(20) Danesi, S.; Porter, R. S. *Polymer* **1978**, *19*, 448.
(21) Lyngaae-Jørgensen, J.; Utracki, L. A. *Makromol. Chem., Macromol. Symp*. **1991**, 48/49, 189.
(22) Sahimi, M. *Applications of Percolation Theory*; Taylor & Francis Ltd: London, 1994; Chapter 2.
(23) Stauffer, D. *Phys. Rep*. **1979**, *54*, 1.

MA010716U